Supplementary Information for "Broadband Sheet Parametric Oscillator towards $\chi^{(2)}$ Optical Frequency Comb Generation via Cavity Phase Matching"

Xin Ni[1], Kunpeng Jia[1], Xiaohan Wang[1], Huaying Liu[1], Jian Guo[1], Shu-Wei Huang[2], Baicheng Yao[3], Nicol ò Sernicola[1,4], Zhenlin Wang[1], Xinjie Lv[1*], Gang Zhao[1*], Zhenda Xie[1*] and Shi-Ning Zhu[1]

[1] *National Laboratory of Solid State Microstructures, School of Physics, College of Engineering and Applied Sciences, and School of Electronic Science and Engineering, Nanjing University, Nanjing 210093, China*

[2] *Department of Electrical, Computer, and Energy Engineering, University of Colorado Boulder, Boulder, CO 80301, United States*

[3] *Key Laboratory of Optical Fiber Sensing and Communications (Education Ministry of China), University of Electronic Science and Technology of China, Chengdu 611731, China*

[4] *Institute for optics, information and photonics, Friedrich Alexander university Erlangen-Nuremberg, Erlangen 91058, Germany*

[*] *Corresponding author. Email:* xiezhenda@nju.edu.cn(Z.D.X.), *Telephone:* +0086-18936027783(Z.D.X.);

Email: zhaogang@nju.edu.cn(G.Z.), *Telephone: 86-25-83593091* (G.Z.);

Email: lvxinjie@nju.edu.cn (X.J.L.), *Telephone:* +0086-15850515914 (X.J.L.);

I. Simulation of the frequency comb generation dynamics

In this simulation, we model the comb generation process in SOPOs with only second order nonlinearity. The light field evolution is simulated through split-step Fourier method [1], which is a pseudo-spectral numerical method to solve nonlinear

partial differential equations, such as the nonlinear Schrödinger equation in our case. An optical parametric oscillation (OPO) process can be treated as the combination of the nonlinear optical interaction and the linear propagation. In the split-step Fourier method, the OPO process is split into small alternating steps, with nonlinear interaction and linear propagation, respectively. While the nonlinear step is calculated in time domain, the linear step is calculated in the time domain, for maximum simulation efficiency, and Fourier transform is performed between steps for continuous simulation.

In an OPO process, a pump photon scatters into two photons with lower frequencies, which are called signal and idler. We can name the electric field of these three light waves E_p, E_s and E_i, respectively. While the E_p is transform limited in the spectral domain, the E_s and E_i spectrum is much broader due to the high cavity phase matching bandwidth. However, we can still define the carrier frequencies ω_p, ω_s and ω_i of all the three light fields, and the spectral broadening is attributed to the temporal modulation over these carrier waves. Here we can have a maximum bandwidth on the order of 10 *THz*, and thus temporal resolution better than 0.1 *ps* is required from the nature of Fourier transform.

For nonlinear transmission process, the split-step Fourier method is adopted to simplify the calculation steps:

$$E_s(z+\Delta h,t) \approx F_T^{-1}\exp\left(\Delta h\widehat{D}\right)F_T\exp\left(\Delta h\widehat{N}\right)E_s(z,t). \quad (1)$$

where Δh is the step length, $\widehat{D}$ is the linear operator representing linear propagation, and $\widehat{N}$ is the nonlinear operator representing nonlinear conversion process.

It is well known that the three-wave nonlinear coupling equations can be expressed as:

$$\begin{aligned}
\left(\frac{\partial}{\partial z}+\beta_p\frac{\partial}{\partial t}+i\frac{\gamma_p}{2}\frac{\partial^2}{\partial t^2}\right)E_p &= -\alpha_p E_p + i\frac{\omega_p d_{eff}}{n_p c}E_s E_i\exp(+i\Delta kz),\\
\left(\frac{\partial}{\partial z}+\beta_s\frac{\partial}{\partial t}+i\frac{\gamma_s}{2}\frac{\partial^2}{\partial t^2}\right)E_s &= -\alpha_s E_s + i\frac{\omega_s d_{eff}}{n_s c}E_p E_i^*\exp(-i\Delta kz), \quad (2)\\
\left(\frac{\partial}{\partial z}+\beta_i\frac{\partial}{\partial t}+i\frac{\gamma_i}{2}\frac{\partial^2}{\partial t^2}\right)E_i &= -\alpha_i E_i + i\frac{\omega_i d_{eff}}{n_i c}E_p E_s^*\exp(-i\Delta kz),
\end{aligned}$$

where the subscripts p, s and i represent for pump, signal and idler, respectively. β is related to the group velocity by $\upsilon = 1/\beta = c/n_g$, where the group index $n_g = n + \omega\frac{\delta n}{\delta\omega}$; and $\gamma = \frac{\delta}{\delta\omega}\left(\frac{1}{v_g}\right)$ is the group velocity dispersion. The frequency dependent refractive index n(ω) of the MgO doped Lithium Niobate n(ω) is derived from Sellmeier equation in Ref. [2], and Δk is the phase-velocity mismatch for the carrier frequencies, which is defined by

$$\Delta k = k_p - k_s - k_i, \tag{3}$$

and the carrier frequencies satisfy the energy conservation

$$\omega_p = \omega_s + \omega_i. \tag{4}$$

Taking the signal field as example, in the linear propagation step:

$$\left(\frac{\partial}{\partial z} + \beta_s\frac{\partial}{\partial t} + i\frac{\gamma_s}{2}\frac{\partial^2}{\partial t^2} + \alpha_s\right)E_s = 0, \tag{5}$$

a coordinate transformation is performed to a reference frame that moves with the speed v_m of the fastest wave among pump, signal and idler.

Performing a Fourier transformation of Eq. (5) into frequency domain, and substituting $\frac{\delta}{\delta t}$ with $i\omega$

$$\left(\frac{\partial}{\partial z} + i\omega\left(\frac{1}{v_s} - \frac{1}{v_m}\right) - i\omega^2\frac{\gamma_s}{2} + \alpha_s\right)E_s = \left(\frac{\partial}{\partial z} - \widehat{D}\right)E_s = 0, \tag{6}$$

where we define the linear transmission operator $\widehat{D}$ for the description of the propagation effect inside crystal.

Considering Eq. (2), the three-wave coupling is simulated in the nonlinear interaction step, which is solved using the nonlinear operator $\widehat{N}$:

$$\widehat{N}E_s = \frac{\partial}{\partial z}E_s = \frac{i\omega_s d_{eff}}{n_s c}E_p E_i^* \exp(i\Delta k z). \tag{7}$$

Thus the field evolution after every step period Δh can be written as

$$\frac{\partial E_s}{\partial z} = [\widehat{N} + \widehat{D}]E_s, \tag{8}$$

which can be solved as:

$$E_s(z + \Delta h, t) \approx F_T^{-1}\exp\left(\Delta h\widehat{D}\right)F_T\exp\left(\Delta h\widehat{N}\right)E_s(z, t). \tag{9}$$

The pump and idler fields can be derived in a similar way.

II. Simulation of the frequency comb generation in the pulse pump case

To simulated the pulsed pump case in our experiment, the pump light is treated as a pulse envelope, with central frequency of Ω_p, and we define the carrier frequencies of signal and idler Ω_s and Ω_i, respectively. The comb-line frequencies that deviate from Ω_s and Ω_i can be considered as results of time modulation over such carrier frequencies. In the Fourier transform of our split-step method, the step size Δh of the electric field evolution is chosen small enough to achieve the over 10THz broadening around Ω_s and Ω_i.

The SOPO consists two mirrors as linear resonator, where M1 is a total reflection mirror and M2 is an output coupler with a reflectivity of r. The nonlinear medium is filled between M1 and M2. The input signal and idler light fields are treated as vacuum quantum noise [5], and pump light field is treated as generalized Gaussian pulse of 10ns full width half maximum. The parametric light can recirculate in the 485.25 μm-thick SOPO for about 1400 times. After each circulattion, the backward intracavity field $\mathrm{E}_c^{'}$ can be related to the forward field by E_c with $\mathrm{E}_c^{'} = E_c \times r + E_{in} \times \mathrm{t}$, and the output filed E_{out} can be derived as $\mathrm{E}_{\mathrm{out}} = E_c \times t + E_{in} \times r$. Here t and r is M2's transmission and reflectivity, satisfying $\mathrm{r}^2 + t^2 = 1$. In our experiment, Q value of the SOPO is measured to be 1.9×10^5, which corresponds to an effective reflectivity of 93.23%, and it is used in the following simulation.

The relative relation between pump frequency and cavity resonance frequency is important for the comb generation. We choose the center of SOPO resonance frequency Ω_C to be close to $\Omega_p/2$, so that the energy conservation can be achieved. Moreover, it is important to slightly detune Ω_C in respective to $\Omega_p/2$ for a coherent comb generation. To achieve the optimal detuning, the influence of nonlinear dynamics on comb noise have been studied in simulation:

$$N_{comb} = 1 - C_{corr}(T) = 1 - \frac{\int r(t)s(t-T)dt}{\sqrt{\int |r(t)|^2 \, dt \int |s(t)|^2 \, dt}} \tag{10}$$

where temporal noise function N_{comb} can be characterized by the cross correlation $C_{\text{corr}}(T)$ between the temporal waveform inside one repetition r(t) and that of another repetition. In the ideal case of a coherent comb generation, the temporal waveform should repeat itself at the repletion time T, which is defined by the recirculating time of the SOPO cavity. By calculating the autocorrelation of the entire waveform, the repletion time T=7.51485ps can be obtained, which is shown in Fig. S1(a) and Fig. S1(b). The cross correlation approaches unitary in this case, and results in a low comb noise.

In the simulation, we scan the pump detuning υ at different pump levels to search for the lowest comb noise, where $\upsilon = \omega_p - 2\Omega_0$ and Ω_0 is the central cavity resonance frequency. We scan the pump energy from 1.4 to 1.8mJ and the lowest comb noise can be achieved when $\upsilon = 22MHz$ at 1.8mJ pump, which is shown in Fig 4a. Under the above conditions, a time frame of 26 repetitions are ploted together for a comparision, as shown in Fig. 4b. It is shown that these waveforms match each other very well. To visually see the residue noise over these repetitions, We define the relative intensity noise *RIN*:

$$RIN = (delta\_I / \bar{I})_{(m,n)} = \frac{I_{(m,n)} - I_{(1,n)}}{\frac{1}{M}\frac{1}{N}\sum_{i=1}^{M}\sum_{j=1}^{N} I_{(i,j)}} \tag{11}$$

The first repetition is used as reference and we calculate the difference between the intensity of the first repetition and others relative to the average intensity. Here, m represents the serial number of repetitions and n indicates the serial number of the points in one repetition. To further characterize the noise level over the larger time scale, we study the RF beat-note of the whole pulse around the repetition frequency. The result in Fig. S1(f) shows a clean RF peak around 133.06GHz, and the linewidth is fit to be 140MHz, which is close to the Fourier transform limit of the pulse envelope.

The SOPO comb spectrum can be simulated by the Fourier transform of the temporal waveform, and it is shown in Fig. 4d. It is interesting to compare the comb

line spacings to the free spectrum range (FSR) of the cavity resonances in such a normal depression SOPO cavity. As shown in Fig. S1(d), we simulated the FSR by filtering a white light using the SOPO cavity (black dots), and the dispersion can cause an FSR change of over 300MHz within the comb span, and this result is in well-agreement with the calculated resonances using Sellmeier equation (red line). However, the comb lines can be pulled over 150MHz away to remain equally spaced (blue dots), and it agrees well with our experiment measurement as described in the main text (green dots).

III. Simulation of the frequency comb generation in the continues-wave pump case

In above simulation, the numerical results match well with our experimental measurement, and reveal the comb generation dynamics in the pulse pump case. As referred in the main text, the continuous pump can further improve the spectral accuracy and reduce the comb noise.

This simulation is still performed by the split-step method as described in Section I. We scan the pump detuning at different pump power for lowest comb noise. Due to the high accuracy of the CW pump case, we have to search for the repetition time by the autocorrelation calculation of the entire waveform in the time domain at each scan. Fig. S2(a) shows the result of such autocorrelation calculation with -193 *MHz* detuning at 12 *kW* pump, and Fig. S2(b) (c) the repletion time T=7.5153ps can be obtained with high accuracy. We plot 266 repetitions of the temporal waveforms under above condition and the result is shown in Fig. S2(d), and it can be found that these waveforms match each other very well. In fact, they are matched so well that we have to visually see them in the relative noise plot in Fig. S2(e), and the relative noise is less than 0.13%.The spectral behavior of the SOPO comb is also studied, and Fig. S2(f) is the simulated comb spectrum, with over 50nm span. We also simulated the comb spectral evolution in the 10^5 round trips, which shows how the comb evolves until stable, as shown in Fig. S2(g).

In conclusion, we have developed a split-step method to simulate the dynamics of the frequency comb generation in $\chi^{(2)}$ sheet-like μOPO. The simulation result shows that the comb generation with pristine line spacing can be achieved with only second-order nonlinearity, which supports our experimental results. Further investigation in the CW-pump case reveals that high quality comb is possible from such $\chi^{(2)}$ SOPOs, and it is a new approach for the micro-resonator comb study.

FIFURE

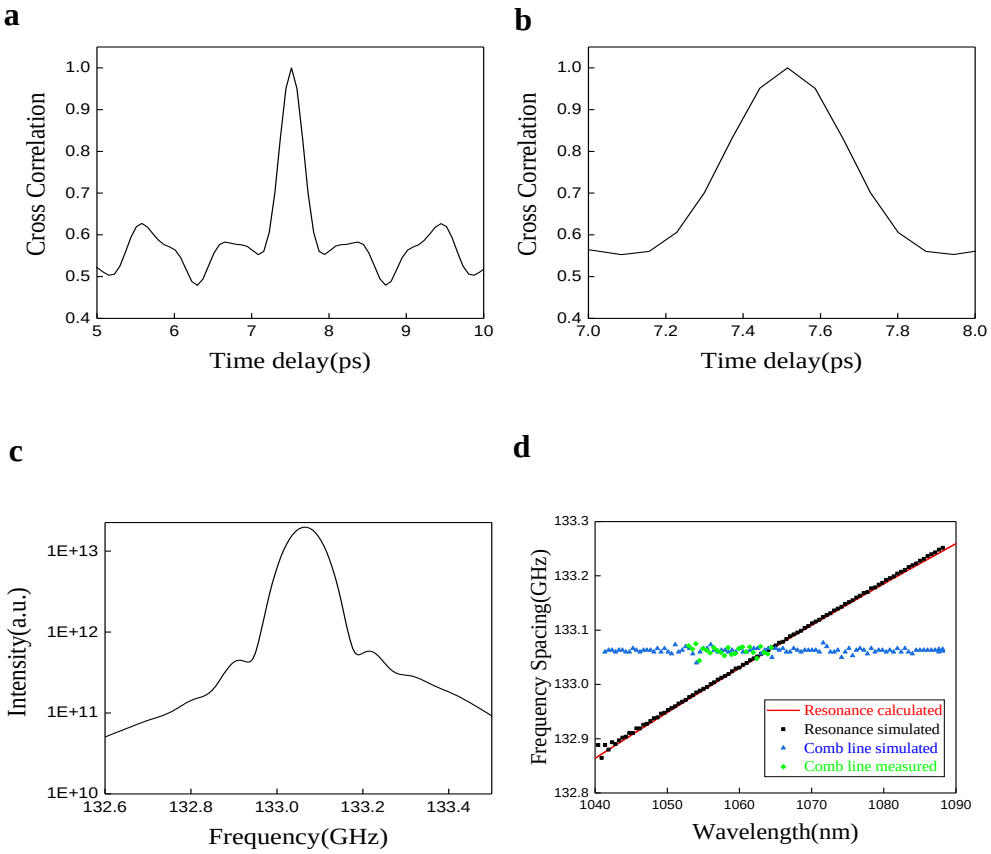

Supplementary Figure S1 | The simulation of the comb generation under pulse pump. **a.** Autocorrelation of the whole time domain waveform**. b.** Zoom in the autocorrelation of the whole time domain waveform and achieve the repetition period T=7.5153ps. **c.** The beat-note spectrum of the first RF peak. **d.** The comparison of the comb line spacing to the cavity resonances.

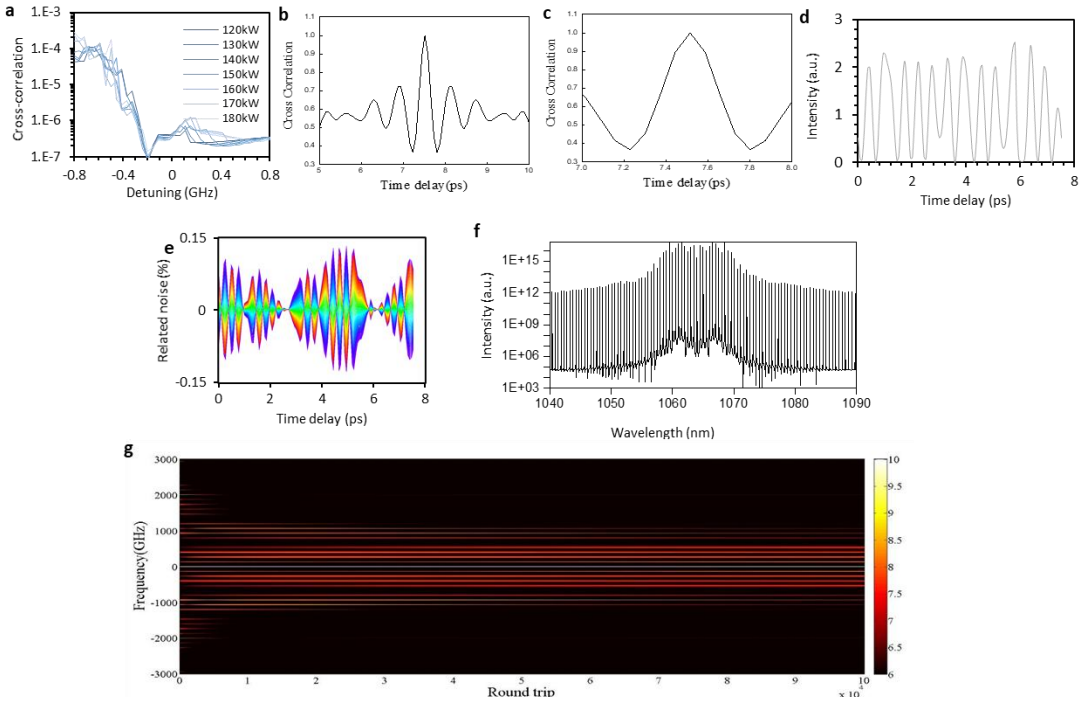

Supplementary Figure S2 | The simulation of the comb generation under CW pump. a. The noise level as a function of pump detuning at different pump power. The lowest noise can be achieved at -193 MHz pump detuning and 12 kW pump, where the spectral and temporal behaviors are studied in detail. **b.** Autocorrelation of the whole time domain waveform**. c.** Zoom in the autocorrelation of the whole time domain waveform and achieve the repetition period T=7.5153ps. **d.** The temporal profiles of 266 repetitions. **e.** The relative intensity noise of 266 repetitions. **f.** The output spectrum of continue wave pump. **g.** The corresponding spectral evolution map.

Supplementary References

[1] Smith A V, Gehr R J, Bowers M S. Numerical models of broad-bandwidth nanosecond optical parametric oscillators. J. Opt. Soc. Am. B 1998; 16**:**609-19

[2] Gayer O, Sacks Z, Galun E, et al., Erratum to: Temperature and wavelength dependent refractive index equations for MgO-doped congruent and stoichiometric $LiNbO_3$. Appl. Phys. B 2010; 101:481.